

Nanostructured Superconductors

Wolfgang Lang^a

^aUniversity of Vienna, Faculty of Physics, Boltzmannngasse 5, Vienna, 1090, Austria

Abstract

The relevant length scales for superconductivity are of the order of nanometers. By confining the superconducting condensate to such dimensions, many physical properties change substantially, and novel phenomena emerge, which are absent in the pristine material. We discuss various methods of creating artificial nanostructures by top-down approaches in metallic and copper-oxide superconductors and their applications. Such nanostructures can be used to control magnetic flux quanta in superconductors, anchoring them to engineered defects to avoid dissipation, guiding their motion, or building artificial flux-quanta arrangements. Nanopatterned superconductors are essential for creating model systems for basic research and enable building almost dissipationless and ultrafast electronic devices and highly sensitive sensors.

Keywords: copper-oxide superconductor, fluxonics, helium ion microscope, high-temperature superconductor, ion irradiation, Josephson effect, lithography, nano-constrictions, nanostructure, pinning lattice, superconductor, vortex, vortex commensurability, vortex ratchet

Contents

1	Introduction	1
2	Nanofabrication techniques	2
2.1	Lithography and ion-beam milling	2
2.2	Electromigration	2
2.3	Templating strategies	3
2.4	Ion-induced nanostructures	3
2.4.1	Masked ion irradiation of thin films	4
2.4.2	Focused ion beam modification of thin films	4
3	Properties of nanopatterned superconductors	5
3.1	Vortex pinning arrays	5
3.2	Complex pinning landscapes	7
3.3	Vortex ratchets and flux diodes	8
3.4	Guided vortex motion	8
3.5	Josephson junctions	9
4	Conclusions and outlook	9
	References	10

This author-created manuscript version is made available under the [CC-BY-NC-ND 4.0 license](https://creativecommons.org/licenses/by-nc-nd/4.0/). The version of record is available at <https://doi.org/10.1016/B978-0-323-90800-9.00014-7>. © 2024 Elsevier.

Cite as: W. Lang, “Nanostructured Superconductors,” in T. Chakraborty (Ed.), *Encyclopedia of Condensed Matter Physics* (Second Edition). Academic Press, Oxford, 2024, pp. 368–380.

Email address: wolfgang.lang@univie.ac.at (Wolfgang Lang)

1. Introduction

Superconductivity originates from the long-range coherence of bosonic quantum particles that condense into a lower energy state and is thus called a macroscopic quantum phenomenon. One might wonder what could be the advantage of confining the superconducting condensate to the nanoscale? The answer lies in two essential characteristic lengths that characterize superconductivity. The Ginzburg-Landau coherence length ξ determines the distance over which the density of superconducting carriers can change from its peak value to zero and vice versa. The size of ξ can vary from several tens of nm in metallic superconductors down to about 1 nm in the copper-oxide superconductors with high critical temperature T_c (HTS). The other length scale is set by the London penetration depth λ , which describes the decay of an external magnetic field from the edge of a superconductor toward its interior, from which it is ultimately expelled.

The ratio between these two lengths bifurcates between two types of superconductors. While so-called type-I superconductors expel a magnetic field completely (Meissner effect), the more abundant and more widely used type-II superconductors let the magnetic field enter in quantized portions of the magnetic flux $\Phi_0 = h/(2e)$, where Φ_0 is termed the flux quantum, h and e are Planck’s constant and the elementary charge, respectively. These flux quanta in a superconductor are called fluxons or vortices; the latter name results from the fact that circular supercurrents in the surrounding material stabilize these flux quanta.

Coming back to the two characteristic lengths, it turns out that the so-called Ginzburg-Landau parameter, the ratio $\kappa = \lambda/\xi$, determines the type of a superconductor, with $\kappa \geq 1/\sqrt{2}$ leading to type-II superconductivity. Another important observation is the temperature dependence of $\xi(T) = \xi(0)(1 -$

$T/T_c)^{-1/2}$ which implies a diverging enhancement of $\xi(T)$ from its minimal value $\xi(0)$ at $T = 0$ when T_c is approached. Ginzburg-Landau theory also predicts the same temperature dependence also for $\lambda(T)$ and, thus, κ is temperature-independent near T_c .

In what follows, we will mainly discuss thin films of superconductors. In many situations, these can be considered three-dimensional (3D) materials, as long as the coherence length perpendicular to the surface is smaller than the film's thickness t_z . However, from the temperature dependence of $\xi(T)$ it is evident that close to T_c a transition to a two-dimensional (2D) behavior in very thin films might occur when $\xi(T) > t_z$.

Another issue becomes important for film thicknesses $t_z \lesssim \lambda(T)$. Then $\lambda(T)$ has to be replaced by an effective penetration depth (also called Pearl length) $\Lambda(T) = 2\lambda(T)^2/t_z$. Since $\lambda(T)$ (and $\Lambda(T)$, respectively) control the range of interactions between vortices, the relevant length scales can become macroscopic in very thin films. In any case, vortices separated by distances smaller than the (effective) penetration depth will behave as collective ensembles, occasionally termed 'vortex matter'. Note that in a magnetic field applied perpendicular to the surface of a thin superconductor, large demagnetization effects lead to a complete penetration of the magnetic flux and to suppression of the Meissner screening.

Vortex physics is a fascinating and complex field of research, and only an introductory glimpse can be presented here to underpin the key issues related to nanostructured superconductors. For deeper insights, see [Brandt \(2024\)](#) in this Encyclopedia and the review by [Blatter et al. \(1994\)](#).

Confining the superconducting condensate to the range of the length scales introduced above inevitably means that superconductors need to be structured to dimensions of few- μm and, primarily, to the nanoscale. The use of thin films and lateral nanostructuring allows one to substantially change many physical properties and create novel phenomena, absent in the pristine material. For example, the controlled manipulation of vortices by anchoring them to engineered defects, guiding their motion, or building artificial vortex matter plays a significant role. Engineered vortex systems are essential for creating model systems for basic research and enable to build almost dissipationless and ultrafast electronic devices based on vortex manipulation, the so-called fluxonics.

Taking advantage of Josephson effects in weakly-coupled superconductors requires barriers of only a few nm in width. The Josephson junction is the central building block for sensitive magnetic field sensors, rapid single flux quantum logic circuits, THz frequency generators, and, last but not least, superconducting quantum computing.

This chapter focuses on the nanostructuring of HTS, which offer easy operation using cryocoolers or liquid nitrogen. However, the brittle nature and complex crystallographic structures of HTS make the fabrication of nanopatterns a problematic endeavor and call for new techniques. Many of these concepts have been developed since the first edition of this Encyclopedia. For a detailed overview of nanostructured metallic superconductors, the reader is referred to the book of [Moshchalkov and Fritzsche \(2011\)](#).

2. Nanofabrication techniques

2.1. Lithography and ion-beam milling

The standard techniques for nanopatterning of superconductor structures focus on thin-film processing. One of the most commonly used methods is photo- or electron-beam lithography, which is well-known for the fabrication of semiconductor devices. After growing thin films on a suitable substrate and depositing a photoresist layer on top, the planar structures are defined by illuminating the photoresist through a mask or directly processing it with an electron-beam (e-beam) writer. While the wavelength of the light limits the former method, e-beam lithography can provide resolutions at the order of 10 nm but is a slow sequential technique.

Unfortunately, the subsequent etching processes of both photoresist and the superconductor result in significant degradation of resolution. Another issue is that etching artifacts, such as underetching below the photoresist layer, progressively limit resolution as the thickness of the superconducting film increases. Thus, patterns in metallic superconductors are generally reported with lateral structures on the order of 100 nm. For example, a vibrant application is the fabrication of single photon detectors ([Gol'tsman et al., 2001](#)) that commonly consist of few-nm thick NbN or NbTiN films patterned to long stripes, folded into meandering patterns to increase the active area ([Hadfield, 2009](#)). The above limitations are of particular importance for the reproducible fabrication of constriction-type Josephson junctions (Dayem bridges), for which a resolution of a few nanometers would be required.

For HTS, the situation is even more complicated because they are brittle and have a complex crystallographic structure. Lithographic techniques combined with etching steps have been successfully applied to create patterns with several hundred nanometers features sizes ([Castellanos et al., 1997](#)). The combination of e-beam lithography followed by argon-ion milling allowed the production of patterns with a minimum line width of 25 nm ([Sochnikov et al., 2010](#)). Since this is still too large to fabricate Josephson junctions directly, alternative fabrication methods, such as growing the thin film over a step-edge in the substrate, must be employed ([Tafari and Kirtley, 2005](#)).

2.2. Electromigration

An elegant way to further narrow the cross-section of superconductor bridges fabricated by conventional lithography is based on electromigration. This usually undesirable process, combining a local temperature rise and a high electric field, leads to a displacement of atoms from their original crystal-lattice positions. Closed-loop controlled electromigration, however, can avoid adverse effects. With the gradual reduction of the cross-section of aluminum constrictions to $\lesssim 150 \text{ nm}^2$, a geometry-induced transition from thermally-assisted phase slips to quantum phase slips has been reported ([Baumans et al., 2016](#)). Other applications of electromigration include the tuning of Nb superconducting quantum interference devices (SQUIDs) ([Collienne et al., 2021](#)) and the controlled migration of oxygen atoms in $\text{YBa}_2\text{Cu}_3\text{O}_7$ (YBCO) bridges ([Marinković et al., 2020](#)).

2.3. Templating strategies

In bottom-up fabrication methods, the nanostructures are already predefined during the growth process. Since patterning the substrate material is often less challenging, several methods have been developed that take advantage of the controlled imperfection in the substrate to introduce the desired structures into the superconductor. One example is the self-organized growth of highly ordered porous alumina, a membrane-like system consisting of triangular arrays of pores. A superconducting Nb thin film deposited directly on the alumina template with a pore spacing of 50 nm acts as a nanoscale array for vortex pinning (Vinckx et al., 2007).

Nanowires of metallic superconductors less than 10 nm in diameter and up to 1 μm in length can be fabricated by ‘molecular templating’ (Bezryadin et al., 2000). After a freestanding carbon nanotube is placed over a narrow and deep slit in a Si substrate, a superconductor such as MoGe is sputtered onto the entire arrangement. The resulting layer consists of the electrodes connected by the nanowire, which are all made of the same material and thus have excellent contact resistances. Subsequently, the properties of the nanowire can be further fine-tuned in a transmission electron microscope or by applying voltage pulses.

Another technique uses vicinally cut substrates with a periodic nanoscale step structure of the clean substrate surface. YBCO films grow on such substrates in a roof-tile-like arrangement of the copper-oxide layers by self-assembly. The morphology and microstructure of such vicinal films strongly depend on the miscut angle of the SrTiO₃ substrate and the thickness of the on-top grown YBCO (Haage et al., 1997; Pedarnig et al., 2002), Bi₂Sr₂CaCu₂O₈ (Durrell et al., 2000), and Hg_{1-x}Re_xBa₂CaCu₂O_{6+ δ} (Re: rare earth element) (Yun et al., 2000) films. The linear arrangement of dislocations resulting from the step structure in YBCO leads to an exceptionally high critical current density. Moreover, symmetry breaking in such vicinal films also allows experimental access to out-of-plane properties of HTS, such as resistivity, Hall effect (Heine et al., 2021), photoconductivity (Markowitsch et al., 1997), and channeling of vortex strings along the *ab*-plane (Berghuis et al., 1997).

Strategies based on substrate modification are very versatile. Nanostructures can be deposited on the substrate prior to the deposition of a superconductor film to modify its structural and superconducting properties. A variety of interactions can be tailored with thickness modulation of the superconductor by insulating dots, proximity effects caused by metallic dots, or magnetic interactions with ferromagnetic dot arrays that interact with the vortex lattice in the superconductor (Martin et al., 1997).

2.4. Ion-induced nanostructures

The previously discussed patterning techniques have several disadvantages, especially when applied to HTS. First, all methods that remove material result in open side faces of the HTS, allowing the relatively mobile oxygen ions to escape from the

crystallographic framework and thus lowering the oxygen content. In most cases, this leads to a degradation of the superconducting properties. On the other hand, the brittle nature of HTS limits the stability of the remaining material structures, making it challenging to achieve sub- μm resolution.

Irradiation of HTS with electrons, protons, and light or heavy ions provides an alternative route to modify the properties of HTS while leaving the surface of the material nearly intact. Before going into further details, a brief account of the limiting parameters is in order. A first consideration concerns the penetration range of irradiation. Only neutrons and high-energy ions can penetrate deeply enough into bulk materials (Weber, 2003). Irradiation with swift heavy ions produces columnar tracks of a few nm diameters in the HTS. The crystallographic structure is destroyed, and a non-superconducting amorphous channel remains (Civale, 1997). Such a columnar defect with a diameter similar to the in-plane coherence length is ideal for blocking the motion of vortices. This enhanced pinning of vortices leads to a higher critical current. These disordered arrangements of line-shaped pinning centers are not only very important for applications but have also triggered the theoretical and experimental study of novel phases of vortex matter, such as the vortex (Fisher et al., 1991) and Bose (Nelson and Vinokur, 1993) glasses.

A more subtle method of tailoring superconducting properties is to create point defects while leaving the crystallographic framework intact. They can be produced by irradiation with electrons, protons, or light ions. Point defects are imperfections at the atomic level that occur when the energy transfer from the incident particle to the crystal is on the order of the energy required to form vacancies. At energies up to a few MeV, the incident particle collides with and displaces a nucleus, eventually creating a collisional cascade that propagates through the material. The tradeoff in the choice of parameters stems from the fact that lighter particles, such as electrons, require extremely high fluence to achieve any appreciable change of the superconducting properties. In contrast, heavier particles have limited penetration depths and more significant scattering of the collisional cascades (Lang and Pedarnig, 2010).

A suitable candidate for the controlled fabrication of point defects in thin films of the most commonly used HTS, YBCO, are He⁺ ions of moderate energy. The superconducting properties are tailored by displacing mainly oxygen atoms, which are more loosely bound than the other atomic species, with binding energies of 1...2 eV for the chain atoms O1 and about 8 eV for the O2/O3 atoms in the CuO₂ planes, as shown in Fig. 1(a). Their displacement creates Frenkel defects at interstitial positions (Gray et al., 2022) outlined in Fig. 1(b), leading to a controllable decrease (Sefrioui et al., 2001) or complete suppression of T_c (Lang and Pedarnig, 2010), depending on the ion fluence. Since the charge transfer from the displaced atoms is still operational, Frenkel defects do not lead to a significant change in the carrier density.

Another process is responsible for reducing T_c : In classical superconductors with *s*-wave symmetry of the superconducting gap, the introduction of point defects has little effect on T_c and is even used technically to improve the critical current. In con-

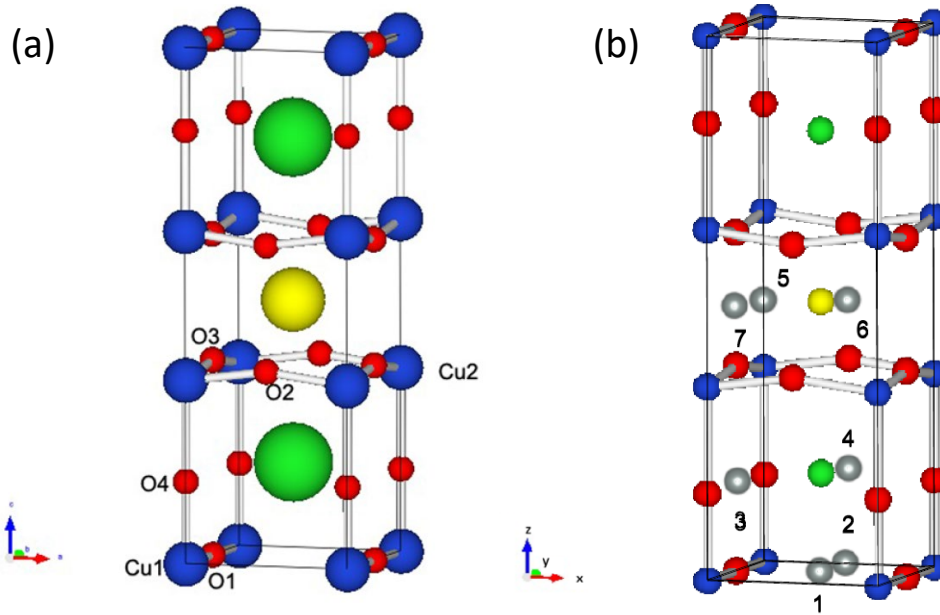


Figure 1: (a) The crystal structure of the copper-oxide superconductor $\text{YBa}_2\text{Cu}_3\text{O}_7$. Red, blue, green, and yellow spheres correspond to oxygen, copper, barium, and yttrium. (b) The gray spheres illustrate possible interstitial sites. Figures reproduced from Gray RL, Rushton MJD, Murphy ST (2022) Molecular dynamics simulations of radiation damage in $\text{YBa}_2\text{Cu}_3\text{O}_7$. *Superconductor Science and Technology* **35**: 035010. doi:10.1088/1361-6668/ac47dc under the [Creative Commons Attribution 4.0](https://creativecommons.org/licenses/by/4.0/) licence.

trast, the anisotropic d -wave nature of the gap in HTS makes it susceptible to tiny defects that reduce not only the normal-state conductivity and carrier mobility but also T_c (Lang and Pedarnig, 2010).

However, a uniform statistical distribution of point defects is not very helpful. By focusing the ion beam before it hits the surface of the HTS film, one can create nearly cylindrical domains populated with point defects. These columnar defects (CDs) form a landscape where superconductivity is locally suppressed. Lateral modulation of ion fluence can be achieved mainly by two different methods outlined in Fig. 2.

2.4.1. Masked ion irradiation of thin films

An extensive array of multiple ion beams can be created by masking a wide-field collinear ion beam, which is commonly available with ion implanters, as schematically shown in Fig. 2(a). An HTS film, thinner than the ion's penetration depth, is fabricated on a suitable substrate. The mask protects selected areas of the HTS film from irradiation and exposes the other sample parts to irradiation. While the former remain superconducting, the T_c of the latter is reduced or suppressed depending on the applied ion energy and fluence. Notably, the collision cascades widen due to the straggling of ion trajectories within the HTS so that the mask patterns become blurred with increasing depth. As a result, the lateral resolution is typically limited to about 10 nm as indicated by simulations with 75 keV He^+ irradiation (Haag et al., 2014).

Different techniques were used to create the mask. Either a photoresist layer was deposited on the HTS and processed with standard UV (Kahlmann et al., 1998), e-beam, (Swiecicki et al., 2012), or focused ion beam (Katz et al., 2000) lithography, then etched and used as the mask, or a metal layer was deposited di-

rectly on the YBCO film and then patterned by ion beam milling (Kang et al., 2002). Alternatively, a Si stencil mask is fabricated and mounted at a small distance from the superconductor film (Lang et al., 2006). This method allows the mask to be reused, does not require the multiple processing steps associated with photoresist, and avoids potential surface degradation.

The main advantage of masking techniques is the parallel processing of many structures. Shortcomings are the resolution limitations resulting from the preparation of the mask, and in the case of freestanding masks, there are geometrical limitations, e.g., disconnected blocking elements are not possible.

2.4.2. Focused ion beam modification of thin films

In contrast to conventional focused ion beam (FIB) machines, which use Ga to ablate the material, devices for focused ion irradiation with light ions have only recently become available. The helium ion microscope (HIM) (Ward et al., 2006) combines scanning focused ion beam sources for He^+ and Ne^+ ions and imaging via secondary electron detection. The HIM consists of a gas-field ion source that emits ions from a tip containing only three atoms (the trimer), electrostatic ion optics to focus and trim the beam, and a deflection system that moves the beam across the sample stage with optional blanking (Fig. 3). Because of the high source brightness of the trimer and the short de Broglie wavelength of He^+ ions, an image resolution better than 0.5 nm and an unprecedented depth of focus can be achieved (Hlawacek and Götzhäuser, 2016).

Using a He or Ne beam instead of the conventional Ga-FIB technique, contamination of the target material by Ga ions is avoided and achieves higher lateral resolution. For example, nanopores as small as 1.3 nm in diameter have been fabricated in 1 nm-thick carbon nanomembranes (Emmrich et al.,

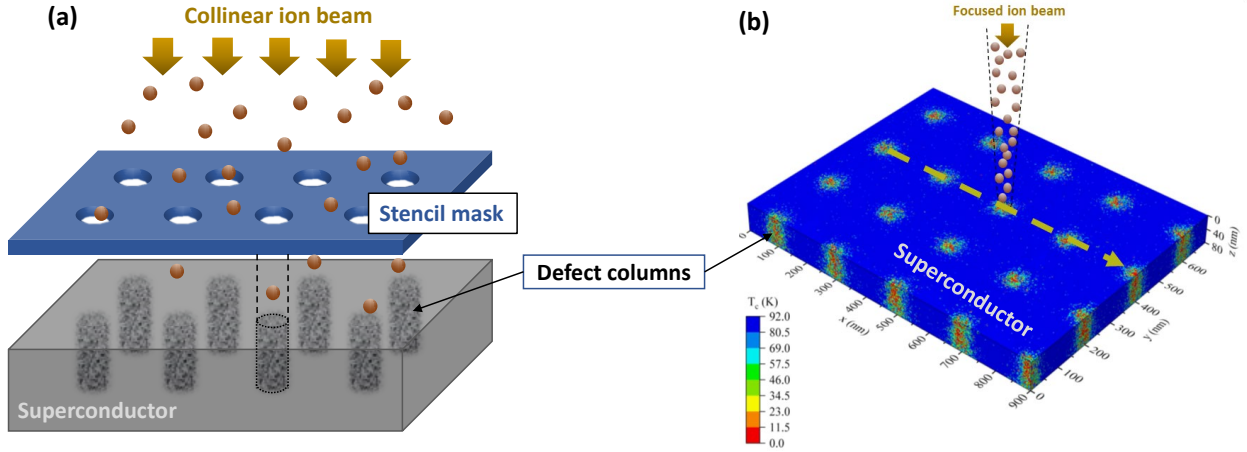


Figure 2: Two different methods for patterning a YBCO film by He^+ ion irradiation: (a) Ion beam patterning through a stencil mask produces a large number of columnar defects in a single step. The dark areas indicate the defect-rich, non-superconducting nanocylinders. (b) Irradiation with a slightly defocused beam from a helium-ion microscope produces tailored columnar defect patterns by scanning the beam across the sample surface. The colors of the columnar defects indicate the local critical temperature, as determined by simulations. Adapted from Aichner B, Mletschnig KL, Müller B, Karrer M, Dosmailov M, Pedarnig JD, Kleiner R, Koelle D, Lang W (2020) Angular magnetic-field dependence of vortex matching in pinning lattices fabricated by focused or masked helium ion beam irradiation of superconducting $\text{YBa}_2\text{Cu}_3\text{O}_{7-\delta}$ thin films. *Low Temperature Physics* 46: 331–337. doi: 10.1063/1.50000863. *Fiz. Nizk. Temp.* 46: 402–409.

2016). As initial applications in HTS, thin barriers of insulating material, written across prepatterned YBCO microbridges with the focused ion beam, form Josephson junctions (Cybart et al., 2015), and ultradense arrays of CDs build a complex pinning landscape for vortices (Aichner et al., 2019). At the time of writing, hexagonal arrays of CDs with spacings as small as 20 nm had been fabricated in YBCO thin films (Karrer et al., 2023).

The use of He–FIB relies on the weak bonding of oxygen in HTS and cannot be employed in the same way for other superconductors. However, a focused Ne beam offers a compromise between Ga–FIB and He–FIB for direct milling of metallic superconductors. This has been demonstrated, for example, for patterning constrictions in NbN films to form nanowires (Burrnett et al., 2017).

Other techniques for growing superconductor nanostructures using focused electron and ion beams are discussed in this Encyclopedia by Córdoba (2024), and the properties of superconducting microtubes and nanohelices are examined by Fomin (2020).

3. Properties of nanopatterned superconductors

Nanostructuring of superconductors enables selective tailoring of the superconducting condensate on length scales smaller than the London penetration depth, mainly by creating lateral structures. Such patterns allow controlled interaction of vortices, their manipulation, as well as tunneling effects between two superconducting condensates weakly coupled by a small non-superconducting interlayer. Some of these applications are described below.

3.1. Vortex pinning arrays

Lateral nanostructuring of superconducting films with regular arrays of CDs allows the creation of artificial pinning land-

scapes that lead to commensurability effects with the flux line lattice. This occurs at the so-called matching fields $B_k = k\Phi_0/A$, where k is an integer number of pinning sites (or a rational number of vortices) in the unit cell of the pinning array of area A . For square lattices $A = a^2$ and for hexagonal patterns $A = \sqrt{3}a^2/2$ with a the nearest neighbor spacing of the CDs.

The number of flux quanta that can be trapped inside a cylindrical hole or in a non-superconducting pinning site depends on its diameter r_p and the coherence length $\xi(T)$ of the superconductor. For anisotropic layered materials such as HTS, the in-plane coherence length $\xi_{ab}(T)$ is relevant. Once all pinning sites are filled by one flux quantum, the formation of multi-quantum vortices becomes energetically favorable when r_p exceeds a certain critical radius (Buzdin, 1993). The saturation number of trapped flux quanta can be estimated by $n_S \approx r_p/2\xi(T)$ (Buzdin and Feinberg, 1996).

A special situation arises for blind holes in a superconductor, i.e., holes that do not completely penetrate the material. The remaining superconducting bottom layer carries the screening currents of individual vortices trapped in the blind hole. Although several flux quanta are trapped in the blind hole, individual vortices can still be made visible (Bezryadin et al., 1996).

Multi-quantum vortices are a phenomenon that occurs only in nanostructured superconductors and does not exist in pure homogeneous superconductors. Conversely, when small pinning sites cannot accommodate the total flux, the excess flux is forced to enter the material via interstitial vortices. The various commensurability effects in a pinning landscape for different magnetic fields applied orthogonally to the film surface are illustrated in Fig. 4, which is based on experimental results by Lorentz microscopy of vortices in a Pb film patterned with a square array of tiny blind holes. For filling factors $k < 1$, the flux quanta are arranged in a superlattice with respect to the pinning array; for $k = 1$, each hole is filled with precisely one

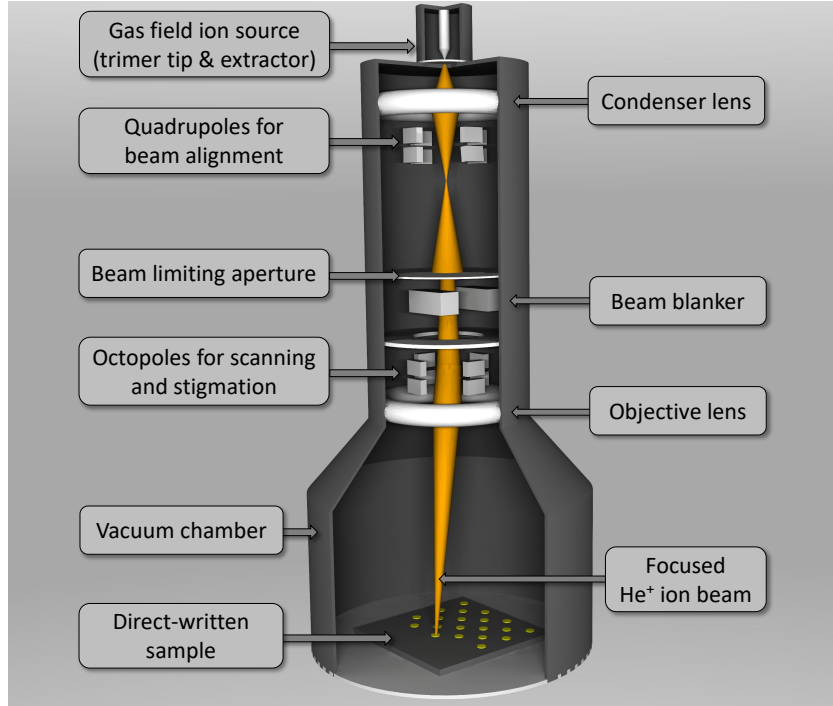


Figure 3: Schematic drawing of the helium ion microscope used for direct-writing patterns of locally suppressed superconductivity. (Courtesy of Bernd Aichner, University of Vienna)

flux quantum, and for $k = 2$, the excess flux is taken up by interstitial vortices.

The commensurability effects manifest themselves in various physical parameters, such as steps in the magnetization loops and peaks in the critical current as indicators of enhanced pinning forces. Minima in the resistance versus magnetic field curves point to commensurability effects of moving vortex ensembles.

Fig. 5 shows an example of the dramatic change of the magnetization loop $M(H)$ after perforating a 60 nm-thick WGe film with a square array of holes 340 nm in diameter and 1 μm apart (Moshchalkov et al., 1996). The area of the $M(H)$ loop in the perforated film is massively increased due to the holes acting as artificial pinning centers. Distinct cusps in the loop appear at the matching fields $B_k = k \times 2.07$ mT, indicating the trapping of multiquanta vortices. The staircase-like reduction of $M(H)$ with increasing field results from the few excess vortices that appear after filling the holes with k vortices. These are initially repelled by the trapped vortices and can move in the interstitial region with higher mobility. As soon as the number of the excess vortices is large enough, they fill up the holes to $k + 1$ multiquanta vortices.

When the diameter of holes in a superconducting film is increased to a size close to their spacing, a gradual change from a pinning lattice to a multiply connected network of superconducting wires takes place. Such wire networks exhibit a modulation of the critical temperature with the magnetic flux, the Little-Parks effect (Parks and Little, 1964). A further enlargement of the holes leads to the formation of disconnected superconducting islands with intriguing properties (Poccia et al.,

2015).

In HTS, commensurability effects can be preferably detected by electric transport measurements, e.g., in YBCO thin films patterned with a square lattice of holes (Castellanos et al., 1997). However, the situation is more complicated because YBCO thin films have strong inherent pinning by crystallographic microtwinning, screw dislocations, and other intrinsic defects. The competition between pinning on these imminent defects and trapping vortices on engineered pinning sites requires that the latter be relatively dense, with a spacing of $\lesssim 300$ nm. Such a resolution is hard to achieve by lithographic methods but is within reach of masked or focused ion beam modification, which can raise the magnitude of the matching fields into the range of several tesla.

A demonstration of vortex commensurability effects at high magnetic fields is shown in Fig 6(a) in a YBCO film with a dense hexagonal pinning lattice with $a = 30$ nm spacing. Since a is much smaller than the Pearl length $\Lambda(0)$, peaks in the critical current caused by enhanced pinning of vortices can be observed at temperatures far below the superconducting transition. Matching effects of mobile vortices at higher temperatures can be traced as dips in the resistivity, as shown in Fig. 6(b). Moreover, the preferential trapping of vortices within the CDs can be confirmed by tilting the applied magnetic field away from the axes of the CDs by an angle α as illustrated in the inset of Fig. 6(b). Then, the position of the matching dips scales with the magnetic field component parallel to the axes of the CDs. These effects prevail up to high tilt angles of $\alpha \leq 70^\circ$ (Aichner et al., 2020).

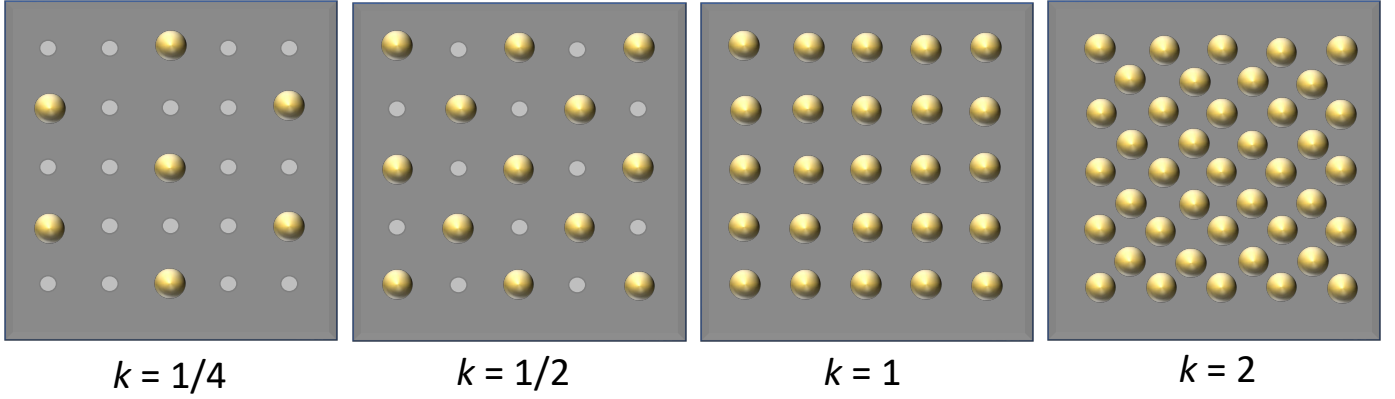


Figure 4: Schematic representation of different commensurability patterns observed by Lorentz microscopy. Light gray circles represent holes in the superconducting film and yellow bullets represent the magnetic flux quanta as observed by a deflection of the electron beam. After Harada et al. (1996).

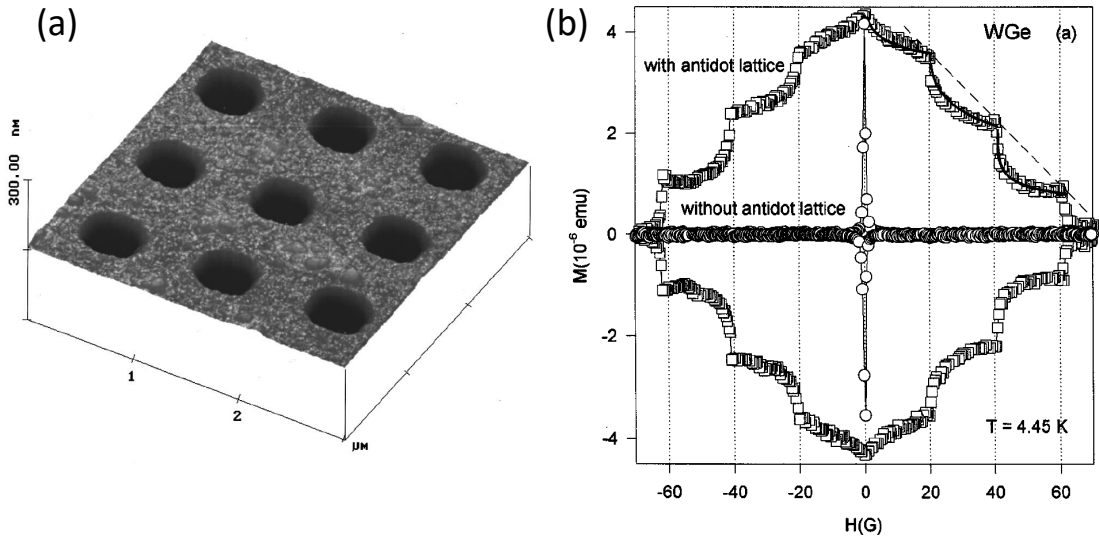


Figure 5: (a) Atomic force microscopy image of a 60 nm-thick WGe film with a square lattice of holes (antidots) with 340 nm diameter and 1 μm spacing. (b) Magnetization loop $M(H)$ at $T = 4.45$ K of the WGe films with and without the antidot grid. The dotted vertical lines indicate the matching fields B_k , $k = 1, 2, 3$. Figures reprinted with permission from Moshchalkov VV, Baert M, Metlushko VV, Rosseel E, Bael MJV, Temst K, Jonckheere R and Bruynseraede Y (1996) *Physical Review B* 54: 7385. Copyright 1996 by the American Physical Society.

3.2. Complex pinning landscapes

When moving from pinning lattices with hexagonal or square arrangements to more complex periodic or aperiodic tilings, numerous unusual phenomena occur. Some examples are shown in Fig. 7. Such patterns have been studied theoretically (Laguna et al., 2001; Misko et al., 2005; Reichhardt and Olson Reichhardt, 2007; Misko and Nori, 2012) and experimentally in metallic superconductors with holes (Kemmler et al., 2006; Misko et al., 2010; Bothner et al., 2014) and magnetic dots (Villegas et al., 2006; Silhanek et al., 2006; Kramer et al., 2009), like Penrose (Kemmler et al., 2006; Misko et al., 2010), honeycomb (Welp et al., 2002; Latimer et al., 2012) and Kagomé (Cuppens et al., 2011) lattices and artificial vortex ice arrangements in geometrically frustrated pinning lattices (Libál et al., 2009; Latimer et al., 2013; Xue et al., 2018).

In HTS, such studies are more challenging and could be hampered by strong intrinsic pinning. However, complex pinning

structures lead to competition between the pinning forces at the CDs and the elastic energy of the vortex lattice, attempting to restore the natural hexagonal vortex configuration of a clean superconductor. For example, pinning landscapes that force the magnetic flux quanta in an ice-like flux arrangement due to a geometrically frustrated energy landscape can transition to a periodic flux distribution at higher temperatures, thawing the vortex ice (Trastoy et al., 2014).

Another example of a complex pinning landscape, the quasi-Kagomé tiling, shows an unconventional commensurability effect. At elevated temperatures, all pins are occupied by vortices, and one interstitial vortex is magnetically caged in each void of the lattice. The balance between the pinning forces exerted by the CDs and the vortex caging potential can be tuned with the temperature (Aichner et al., 2019). Controlled manipulation of such magnetically confined vortices can pave the way toward fluxonic applications of HTS.

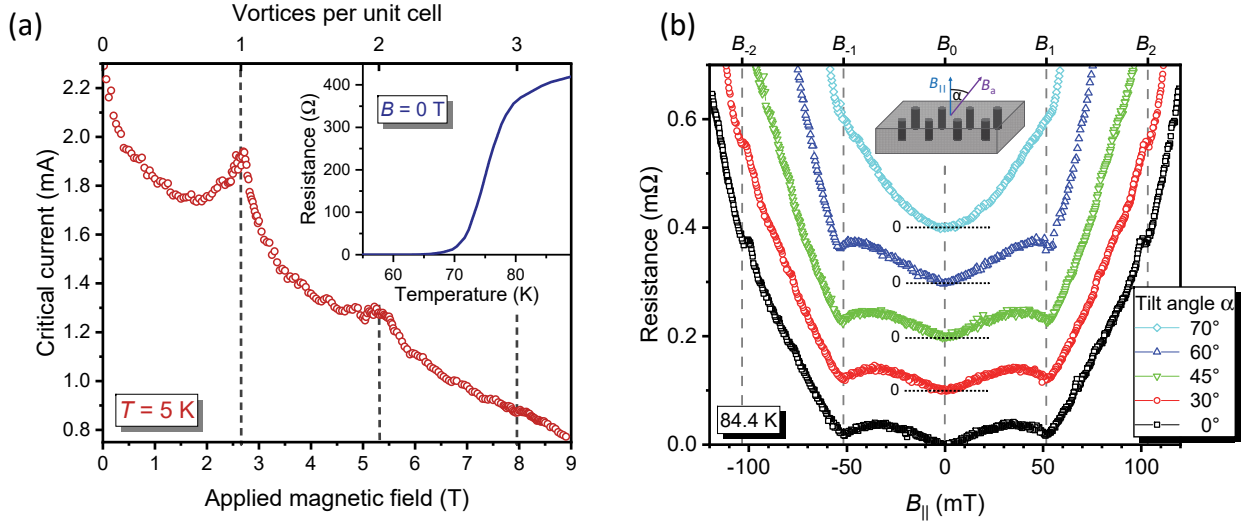


Figure 6: Vortex commensurability effects in YBCO thin films with an array of columnar defects, created by focused He^+ ion beam irradiation. (a) Critical current at 5 K as a function of applied magnetic field of a thin YBCO film with a hexagonal pattern of columnar defects spaced 30 nm apart. At the first matching field $B_1 = 2.65$ T, a peak of the critical current is caused by strong commensurability effects. Another peak occurs when two vortices are trapped in the pins. The inset shows the superconducting transition in zero magnetic field. Adapted from Backmeister et al. (2022). (b) Angular dependence of vortex matching effects in the resistance of a YBCO thin film with a square lattice of 200 nm spaced columnar defects: The resistance is plotted as a function of the applied field component along the normal of the film surface $B_{||} = B_a \cos \alpha$ for different values of α . For $\alpha > 0^\circ$ the curves are shifted by multiples of 0.1 mΩ for better visibility. The inset shows a sketch of the experimental situation. Reprinted with permission from Aichner et al. (2020).

3.3. Vortex ratchets and flux diodes

By introducing spatial asymmetry into the pinning arrays, many exciting effects emerge. In general, the idea of a ‘Brownian motor’ refers to Brownian motion in combination with an unbiased external input signal that can induce submicron directional motion of particles (Hänggi and Marchesoni, 2009). A well-known example is the directional propagation of vortices in an appropriately structured superconductor, usually referred to as a ‘vortex ratchet’ or ‘fluxon pump’ (Wambaugh et al., 1999). It provides a flexible and well-controlled model system for studying stochastic transport processes and can operate up to THz frequencies (Hastings et al., 2003).

Vortex ratchets can be realized by various concepts, such as 2D asymmetric channel walls. They can be further extended to design ‘fluxon optics’ devices, concave/convex fluxon lenses that disperse/concentrate fluxons in nanodevices (Wambaugh et al., 1999). Also, asymmetric potential barriers, e.g., in the form of square arrays of triangular pinning centers (Villegas et al., 2003), double-well traps, (Van de Vondel et al., 2005) or an asymmetric arrangement of symmetric traps, (Wördenweber et al., 2004; Perez de Lara et al., 2010) lead to vortex rectification effects.

Interestingly, ratchet effects are proposed in binary particle mixtures without needing for an asymmetric substrate (Savel’ev and Nori, 2002). For example, in layered superconductors, such as HTS, an inclination of the magnetic field from the c axis leads to a mixture of pancake vortices and Josephson strings. This hybrid vortex system exhibits ratchet effects with time asymmetric drives (Cole et al., 2006).

Finally, understanding ratchet effects in different systems is an exciting topic. Studying these effects with fluxons provides a more direct and controllable experimental approach than most

other systems. Ultimately, these investigations may pave the way to cellular automata as an alternative concept (Hastings et al., 2003; Milošević et al., 2007) for performing clocked logic operations on discrete particles. Moreover, vortex ratchets are proposed (Lee et al., 1999) as an effective method for evacuating magnetic flux from superconducting devices where inadvertently trapped flux might be detrimental for operation, such as in SQUID magnetic sensors.

A related concept is the lossless superconducting diode. This is an electronic device that has zero resistance only for one direction of applied current and is a desirable device for building electronic circuits with ultra-low power consumption. It can be realized as a superconducting film patterned with a conformal array of nanoscale holes that breaks spatial inversion symmetry (Lyu et al., 2021). A conformal array is a structure resulting from the transformation of a uniform hexagonal pinning array that retains the sixfold order of the original lattice but exhibits a gradient in site density (Reichhardt et al., 2015).

3.4. Guided vortex motion

Controlled vortex motion along a predefined path can be achieved by patterning narrow channels or parallel rows of defects into a superconductor. This so-called ‘guided vortex motion’ results from an easy track in which vortex pinning is reduced (Dobrovolskiy et al., 2016), a row of holes (Silhanek et al., 2010), or, in HTS, the suppression of superconductivity by heavy-ion irradiation (Laviano et al., 2010). Guided vortex motion can be detected by the deflection of vortices from their trajectory imposed by the Lorentz force. This leads to a pronounced transverse voltage (Wördenweber et al., 2004) that can be distinguished from the conventional Hall effect by its even symmetry with respect to the reversal of the magnetic

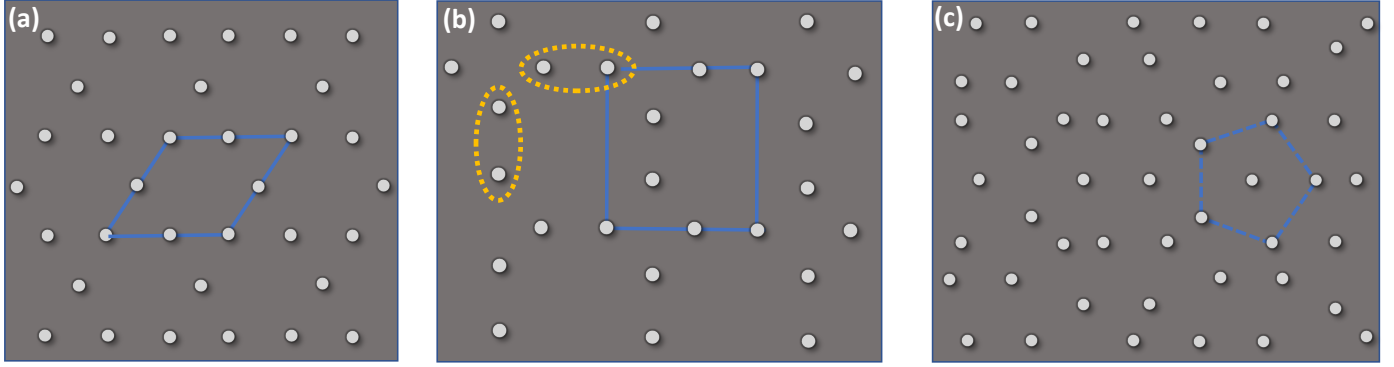


Figure 7: Examples of complex pinning landscapes. Bright circles indicate pinning centers (holes or columnar defects) and solid blue lines the unit cell of a periodic lattice. (a) The Kagomé lattice is related to the hexagonal lattice. The latter can be recovered if one pin is added in the center of each void. (b) Vortex-ice lattice: four pairs of pins (indicated by orange ellipses) meet at each vertex of a square lattice. (c) The aperiodic Penrose tiling. The dashed blue lines indicate the five-fold symmetry.

field. Guided vortex motion also plays an important role in experiments where vortices are accelerated to high velocities, as discussed by [Dobrovolskiy \(2024\)](#).

3.5. Josephson junctions

A ubiquitous need for nanostructuring of superconductors arises from the fabrication of Josephson junctions (JJs), where two superconducting systems are separated by an insulating or metallic barrier of a few nm thickness or by another weak coupling link. It is crucial that the Josephson weak links are stable and can be reproducibly fabricated. While for metallic superconductors the industrial fabrication of circuits based on JJs has been established for many years ([Likharev, 2012](#)), the fabrication of JJs in HTS is much more challenging. It is still in the phase of cumulative progress.

JJs consisting exclusively of HTS materials have been produced by introducing a crystallographic fault (break junctions), by using a grain boundary between different crystallites, by growing thin HTS films over a substrate step, by narrow constrictions (Dayem bridges), or by multilayers forcing the current along the c -axis ([Koelle et al., 1999](#)). Here we restrict ourselves to discussing JJs in HTS produced by masked or focused ion irradiation. A general account of this subject can be found in the chapter by [Tafari \(2024\)](#).

Several attempts have been made to fabricate JJs by irradiation techniques. Initially, direct writing of narrow lines with an electron beam across a pre-patterned YBCO bridge in a scanning electron microscope resulted in somewhat unstable JJs and required high electron doses. Later, creating a weak link in YBCO bridges by implanting oxygen ions through a lithographically defined mask led to superconducting-normal-superconducting (SNS) JJs with resistively shunted junction (RSJ) properties ([Tinchev, 1996](#); [Kahlmann et al., 1998](#); [Bergeal et al., 2005](#)). However, the minimum width of the mask structures of about 20 nm, and the inevitable straggle of ion collision cascades in the YBCO film set resolution limits and prevent fabrication of superconductor-insulator-superconductor (SIS) junctions, which would be the ultimate goal.

A similar technique, but using 200 keV Ne^+ ions, allows complete penetration of the ions through the YBCO film, avoiding implantation and limiting the intended damage to the creation of point defects ([Katz et al., 1998](#)). This technique can be scaled up to integrating of many JJs in a 2D series-parallel array; 15,820 (28×565) JJs have been demonstrated ([Cybart et al., 2009](#)).

Focused He^+ ion irradiation in a HIM took the fabrication of JJs one step further. Tunnel junctions can be directly written with the focused He-ion beam into YBCO films, as illustrated in Fig. 8. The properties of the barrier are controlled by varying the irradiation dose. With this technique, SIS junction can also be realized ([Cybart et al., 2014](#)). Scanning transmission electron analysis shows that the amorphous tracks created by 1500 He^+/nm have a lateral extension of 4 nm, while no destruction of the crystallographic structure is observed at lower fluence. Nevertheless, the devices produced with the lower doses show an explicit JJ behavior ([Müller et al., 2019](#)).

The He-FIB technique can, in principle, be applied to other HTS, as has been demonstrated for $\text{La}_{1.84}\text{Sr}_{0.16}\text{CuO}_4$ ([Gozar et al., 2017](#)) and other superconducting materials such as MgB_2 ([Kasaei et al., 2018](#)). The versatility of directly written structures and JJs provides a tremendous advantage in fabricating superconducting quantum interference devices ([Müller et al., 2019](#)), JJ arrays ([LeFebvre et al., 2019](#)), and even more complex devices on the same substrate for various applications.

4. Conclusions and outlook

In this chapter, we have outlined various methods for fabricating nanostructured superconductors. While established lithographic and ion-milling techniques enable the patterning of metallic superconductors, novel techniques are required for nanoscale structures in copper-oxide superconductors. For example, focused He^+ -ion beam irradiation creates columnar channels of point defects and can be used to create vortex pinning landscapes and weak links for Josephson junctions. Superconducting nanostructures are already indispensable for many

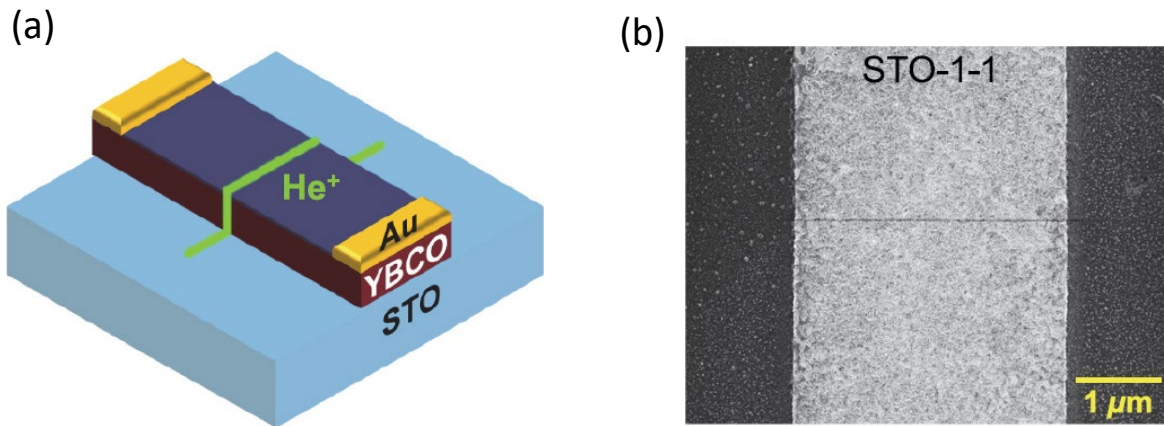


Figure 8: (a) Schematic illustration of a Josephson junction fabricated by focused He^+ ion irradiation in a helium ion microscope. (b) Scanning electron image of the junction (visible as a thin dark line) patterned with a fluence of 600 ions/nm. Figures reprinted with permission from Müller B, Karrer M, Limberger F, Becker M, Schröppel B, Burkhardt CJ, Kleiner R, Goldobin E and Koelle D (2019) *Physical Review Applied* 11: 044082. Copyright 2019 by the American Physical Society.

applications and will bring further significant advances to applications of superconducting electronics, from fluxonics to ultra-high sensitivity magnetometers and many others. Beyond that, the dawning age of superconducting quantum computing depends heavily on precise and reproducible nanostructured circuits on a large scale.

Acknowledgments

This work was supported by the Austrian Science Fund (FWF), grant I4865-N, and is based upon work from COST Actions CA16218 (NANOCOHYBRI), CA19108 (Hi-SCALE), and CA19140 (FIT4NANO), supported by COST (European Cooperation in Science and Technology).

References

Aichner, B., Mletschnig, K.L., Müller, B., Karrer, M., Dosmailov, M., Pedarnig, J.D., Kleiner, R., Koelle, D., Lang, W., 2020. Angular magnetic-field dependence of vortex matching in pinning lattices fabricated by focused or masked helium ion beam irradiation of superconducting $\text{YBa}_2\text{Cu}_3\text{O}_{7-\delta}$ thin films. *Low Temp. Phys.* 46, 331–337. doi:10.1063/1.5000863. *Fiz. Nizk. Temp.* 46, 402–409.

Aichner, B., Müller, B., Karrer, M., Misko, V.R., Limberger, F., Mletschnig, K.L., Dosmailov, M., Pedarnig, J.D., Nori, F., Kleiner, R., Koelle, D., Lang, W., 2019. Ultradense tailored vortex pinning arrays in superconducting $\text{YBa}_2\text{Cu}_3\text{O}_{7-\delta}$ thin films created by focused He ion beam irradiation for fluxonics applications. *ACS Appl. Nano Mater.* 2, 5108–5115. doi:10.1021/acsanm.9b01006.

Backmeister, L., Aichner, B., Karrer, M., Wurster, K., Kleiner, R., Goldobin, E., Koelle, D., Lang, W., 2022. Ordered Bose glass of vortices in superconducting $\text{YBa}_2\text{Cu}_3\text{O}_{7-\delta}$ thin films with a periodic pin lattice created by focused helium ion irradiation. *Nanomaterials* 12, 3491. doi:10.3390/nano12193491.

Baumans, X.D.A., Cerbu, D., Adami, O.A., Zharinov, V.S., Verellen, N., Papari, G., Scheerder, J.E., Zhang, G., Moshchalkov, V.V., Silhanek, A.V., Van de Vondel, J., 2016. Thermal and quantum depletion of superconductivity in narrow junctions created by controlled electromigration. *Nat. Commun.* 7, 10560. doi:10.1038/ncomms10560.

Bergeal, N., Grison, X., Lesueur, J., Faini, G., Aprili, M., Contour, J.P., 2005. High-quality planar high- T_c Josephson junctions. *Appl. Phys. Lett.* 87, 102502. doi:10.1063/1.2037206.

Berghuis, P., Di Bartolomeo, E., Wagner, G.A., Evetts, J.E., 1997. Intrinsic channeling of vortices along the ab plane in vicinal $\text{YBa}_2\text{Cu}_3\text{O}_{7-\delta}$ films. *Phys. Rev. Lett.* 79, 2332–2335. doi:10.1103/PhysRevLett.79.2332.

Bezryadin, A., Lau, C.N., Tinkham, M., 2000. Quantum suppression of superconductivity in ultrathin nanowires. *Nature* 404, 971–974. doi:10.1038/35010060.

Bezryadin, A., Ovchinnikov, Y.N., Pannetier, B., 1996. Nucleation of vortices inside open and blind microholes. *Phys. Rev. B* 53, 8553–8560. doi:10.1103/PhysRevB.53.8553.

Blatter, G., Feigel'man, M.V., Geshkenbein, V.B., Larkin, A.I., Vinokur, V.M., 1994. Vortices in high-temperature superconductors. *Rev. Mod. Phys.* 66, 1125–1388. doi:10.1103/RevModPhys.66.1125.

Bothner, D., Seidl, R., Misko, V.R., Kleiner, R., Koelle, D., Kemmler, M., 2014. Unusual commensurability effects in quasiperiodic pinning arrays induced by local inhomogeneities of the pinning site density. *Supercond. Sci. Technol.* 27, 065002. doi:10.1088/0953-2048/27/6/065002.

Brandt, E.H., 2024. Superconductivity: Ginzburg-Landau theory and vortex lattice, in: Chakraborty, T. (Ed.), *Encyclopedia of Condensed Matter Physics* (Second Edition). Academic Press, Oxford, pp. 693–701. doi:10.1016/B978-0-323-90800-9.00079-2.

Burnett, J., Sagar, J., Kennedy, O.W., Warburton, P.A., Fenton, J.C., 2017. Low-loss superconducting nanowire circuits using a neon focused ion beam. *Phys. Rev. Appl.* 8, 014039. doi:10.1103/physrevapplied.8.014039.

Buzdin, A., Feinberg, D., 1996. Electromagnetic pinning of vortices by non-superconducting defects and their influence on screening. *Physica C* 256, 303–311. doi:10.1016/0921-4534(95)00664-8.

Buzdin, A.I., 1993. Multiple-quanta vortices at columnar defects. *Phys. Rev. B* 47, 11416. doi:10.1103/PhysRevB.47.11416.

Castellanos, A., Wördenweber, R., Ockenfuss, G., v.d. Hart, A., Keck, K., 1997. Preparation of regular arrays of antidots in $\text{YBa}_2\text{Cu}_3\text{O}_7$ thin films and observation of vortex lattice matching effects. *Appl. Phys. Lett.* 71, 962–964. doi:10.1063/1.119701.

Civale, L., 1997. Vortex pinning and creep in high-temperature superconductors with columnar defects. *Supercond. Sci. Technol.* 10, A11–A28. doi:10.1088/0953-2048/10/7a/003.

Cole, D., Bending, S., Savel'ev, S., Grigorenko, A., Tamegai, T., Nori, F., 2006. Ratchet without spatial asymmetry for controlling the motion of magnetic flux quanta using time-asymmetric drives. *Nat. Mater.* 5, 305–311. doi:10.1038/nmat1608.

Collienne, S., Raes, B., Keijers, W., Linek, J., Koelle, D., Kleiner, R., Kramer, R.B.G., Van de Vondel, J., Silhanek, A.V., 2021. Nb-based nanoscale superconducting quantum interference devices tuned by electroannealing. *Phys. Rev. Appl.* 15, 034016. doi:10.1103/physrevapplied.15.034016.

Córdoba, R., 2024. Additive nanofabrication using focused ion and electron beams, in: Chakraborty, T. (Ed.), *Encyclopedia of Condensed Matter Physics* (Second Edition). Academic Press, Oxford, pp. 448–464. doi:10.1016/B978-0-323-90800-9.00035-4.

Cuppens, J., Ataklti, G.W., Gillijns, W., Van de Vondel, J., Moshchalkov, V.V.,

- Silhanek, A.V., 2011. Vortex dynamics in a superconducting film with a kagome and a honeycomb pinning landscape. *J. Supercond. Novel Magn.* 24, 7–11. doi:10.1007/s10948-010-0893-7.
- Cybart, S.A., Anton, S.M., Wu, S.M., Clarke, J., Dynes, R.C., 2009. Very large scale integration of nanopatterned $\text{YBa}_2\text{Cu}_3\text{O}_{7-\delta}$ Josephson junctions in a two-dimensional array. *Nano Lett.* 9, 3581–3585. doi:10.1021/nl901785j.
- Cybart, S.A., Cho, E.Y., Wong, T.J., Glyantsev, V.N., Huh, J.U., Yung, C.S., Moeckly, B.H., Beeman, J.W., Ulin-Avila, E., Wu, S.M., Dynes, R.C., 2014. Large voltage modulation in magnetic field sensors from two-dimensional arrays of Y-Ba-Cu-O nano Josephson junctions. *Appl. Phys. Lett.* 104, 062601. doi:10.1063/1.4865216.
- Cybart, S.A., Cho, E.Y., Wong, T.J., Wehlin, B.H., Ma, M.K., Huynh, C., Dynes, R.C., 2015. Nano Josephson superconducting tunnel junctions in $\text{YBa}_2\text{Cu}_3\text{O}_{7-\delta}$ directly patterned with a focused helium ion beam. *Nat. Nanotechnol.* 10, 598. doi:10.1038/nnano.2015.76.
- Dobrovolskiy, O.V., 2024. Fast dynamics of vortices in superconductors, in: Chakraborty, T. (Ed.), *Encyclopedia of Condensed Matter Physics* (Second Edition). Academic Press, Oxford, pp. 735–754. doi:10.1016/B978-0-323-90800-9.00015-9.
- Dobrovolskiy, O.V., Hanefeld, M., Zörb, M., Huth, M., Shklovskij, V.A., 2016. Interplay of flux guiding and Hall effect in Nb films with nanogrooves. *Supercond. Sci. Technol.* 29, 065009. doi:10.1088/0953-2048/29/6/065009.
- Durrell, J.H., Gibson, G., Barber, Z.H., Evetts, J.E., Rössler, R., Pedarnig, J.D., Bäuerle, D., 2000. Dependence of critical current on field angle in off-c-axis grown $\text{Bi}_2\text{Sr}_2\text{CaCu}_2\text{O}_8$ film. *Appl. Phys. Lett.* 77, 1686–8. doi:10.1063/1.1310174.
- Emmrich, D., Beyer, A., Nadzeyka, A., Bauerdick, S., Meyer, J.C., Kotakoski, J., Götzhäuser, A., 2016. Nanopore fabrication and characterization by helium ion microscopy. *Appl. Phys. Lett.* 108, 163103. doi:10.1063/1.4947277.
- Fisher, D.S., Fisher, M.P.A., Huse, D.A., 1991. Thermal fluctuations, quenched disorder, phase transitions, and transport in type-II superconductors. *Phys. Rev.* 43, 130–159. doi:10.1103/physrevb.43.130.
- Fomin, V.M., 2020. Self-rolled Micro- and Nanoarchitectures. De Gruyter, Berlin/Boston. doi:10.1515/9783110575576.
- Gol'tsman, G.N., Okunev, O., Chulkova, G., Lipatov, A., Semenov, A., Smirnov, K., Voronov, B., Dzardanov, A., Williams, C., Sobolewski, R., 2001. Picosecond superconducting single-photon optical detector. *Appl. Phys. Lett.* 79, 705–707. doi:10.1063/1.1388868.
- Gozar, A., Litombe, N.E., Hoffman, J.E., Božović, I., 2017. Optical nanoscopy of high T_c cuprate nanoconstriction devices patterned by helium ion beams. *Nano Lett.* 17, 1582–1586. doi:10.1021/acs.nanolett.6b04729.
- Gray, R.L., Rushton, M.J.D., Murphy, S.T., 2022. Molecular dynamics simulations of radiation damage in $\text{YBa}_2\text{Cu}_3\text{O}_7$. *Supercond. Sci. Technol.* 35, 035010. doi:10.1088/1361-6668/ac47dc.
- Haag, L.T., Zechner, G., Lang, W., Dosmailov, M., Bodea, M.A., Pedarnig, J.D., 2014. Strong vortex matching effects in YBCO films with periodic modulations of the superconducting order parameter fabricated by masked ion irradiation. *Physica C* 503, 75–81. doi:10.1016/j.physc.2014.03.032.
- Haage, T., Zegenhagen, J., Li, J.Q., Habermeier, H.U., Cardona, M., Warthmann, J.R., Forkl, A., Kronmüller, H., 1997. Transport properties and flux pinning by self-organization in $\text{YBa}_2\text{Cu}_3\text{O}_{7-\delta}$ films on vicinal SrTiO_3 (001). *Phys. Rev. B* 56, 8404–8418. doi:10.1103/PhysRevB.56.8404.
- Hadfield, R.H., 2009. Single-photon detectors for optical quantum information applications. *Nat. Photon.* 3, 696–705. doi:10.1038/nphoton.2009.230.
- Hänggi, P., Marchesoni, F., 2009. Artificial Brownian motors: Controlling transport on the nanoscale. *Rev. Mod. Phys.* 81, 387–442. doi:10.1103/RevModPhys.81.387.
- Harada, K., Kamimura, O., Kasai, H., Matsuda, T., Tonomura, A., Moshchalkov, V.V., 1996. Direct observation of vortex dynamics in superconducting films with regular arrays of defects. *Science* 274, 1167–1170. doi:10.1126/science.274.5290.1167.
- Hastings, M.B., Olson Reichhardt, C.J., Reichhardt, C., 2003. Ratchet cellular automata. *Phys. Rev. Lett.* 90, 247004. doi:10.1103/physrevlett.90.247004.
- Heine, G., Lang, W., Rössler, R., Pedarnig, J.D., 2021. Anisotropy of the in-plane and out-of-plane resistivity and the Hall effect in the normal state of vicinal-grown $\text{YBa}_2\text{Cu}_3\text{O}_{7-\delta}$ thin films. *Nanomaterials* 11, 675. doi:10.3390/nano11030675.
- Hlawacek, G., Götzhäuser, A. (Eds.), 2016. *Helium Ion Microscopy*. Springer International Publishing, Switzerland. doi:10.1007/978-3-319-41990-9.
- Kahlmann, F., Engelhardt, A., Schubert, J., Zander, W., Buchal, C., Hollkott, J., 1998. Superconductor-normal-superconductor Josephson junctions fabricated by oxygen implantation into $\text{YBa}_2\text{Cu}_3\text{O}_{7-\delta}$. *Appl. Phys. Lett.* 73, 2354–6. doi:10.1063/1.122459.
- Kang, D.J., Burnell, G., Lloyd, S.J., Speaks, R.S., Peng, N.H., Jaynes, C., Webb, R., Yun, J.H., Moon, S.H., Oh, B., Tarte, E.J., Moore, D.F., Blamire, M.G., 2002. Realization and properties of $\text{YBa}_2\text{Cu}_3\text{O}_{7-\delta}$ Josephson junctions by metal masked ion damage technique. *Appl. Phys. Lett.* 80, 814–816. doi:10.1063/1.1446998.
- Karrer, M., Aichner, B., Wurster, K., Kleiner, R., Goldobin, E., Koelle, D., Lang, W., 2023. High-magnetic-field commensurability effects in ultradense pinning lattices fabricated by focused He-ion beam. In preparation.
- Kasaei, L., Melbourne, T., Manichev, V., Feldman, L.C., Gustafsson, T., Chen, K., Xi, X.X., Davidson, B.A., 2018. MgB_2 Josephson junctions produced by focused helium ion beam irradiation. *AIP Adv.* 8, 075020. doi:10.1063/1.5030751.
- Katz, A.S., Sun, A.G., Woods, S.I., Dynes, R.C., 1998. Planar thin film $\text{YBa}_2\text{Cu}_3\text{O}_{7-\delta}$ Josephson junctions via nanolithography and ion damage. *Appl. Phys. Lett.* 72, 2032–2034. doi:10.1063/1.121255.
- Katz, A.S., Woods, S.I., Dynes, R.C., 2000. Transport properties of high- T_c planar Josephson junctions fabricated by nanolithography and ion implantation. *J. Appl. Phys.* 87, 2978–83. doi:10.1063/1.372286.
- Kemmler, M., Gürlich, C., Sterck, A., Pöhler, H., Neuhäuser, M., Siegel, M., Kleiner, R., Koelle, D., 2006. Commensurability effects in superconducting Nb films with quasiperiodic pinning arrays. *Phys. Rev. Lett.* 97, 147003. doi:10.1103/physrevlett.97.147003.
- Koelle, D., Kleiner, R., Ludwig, F., Dantsker, E., Clarke, J., 1999. High-transition-temperature superconducting quantum interference devices. *Rev. Mod. Phys.* 71, 631–686. doi:10.1103/revmodphys.71.631.
- Kramer, R.B.G., Silhanek, A.V., Van de Vondel, J., Raes, B., Moshchalkov, V.V., 2009. Symmetry-induced giant vortex state in a superconducting Pb film with a fivefold Penrose array of magnetic pinning centers. *Phys. Rev. Lett.* 103, 067007. doi:10.1103/physrevlett.103.067007.
- Laguna, M.F., Balseiro, C.A., Domínguez, D., Nori, F., 2001. Vortex structure and dynamics in kagomé and triangular pinning potentials. *Phys. Rev. B* 64, 104505. doi:10.1103/PhysRevB.64.104505.
- Lang, W., Dineva, M., Marksteiner, M., Enzenhofer, T., Siraj, K., Peruzzi, M., Pedarnig, J.D., Bäuerle, D., Korntner, R., Cekan, E., Platzgummer, E., Loeschner, H., 2006. Ion-beam direct-structuring of high-temperature superconductors. *Microelectron. Eng.* 83, 1495–1498. doi:10.1016/j.mee.2006.01.091.
- Lang, W., Pedarnig, J.D., 2010. Ion irradiation of high-temperature superconductors and its application for nanopatterning, in: Moshchalkov, V.V., Würdenweber, R., Lang, W. (Eds.), *Nanoscience and Engineering in Superconductivity*. Springer, Heidelberg, pp. 81–104. doi:10.1007/978-3-642-15137-8.
- Latimer, M.L., Berdiyrov, G.R., Xiao, Z.L., Kwok, W.K., Peeters, F.M., 2012. Vortex interaction enhanced saturation number and caging effect in a superconducting film with a honeycomb array of nanoscale holes. *Phys. Rev. B* 85, 012505. doi:10.1103/PhysRevB.85.012505.
- Latimer, M.L., Berdiyrov, G.R., Xiao, Z.L., Peeters, F.M., Kwok, W.K., 2013. Realization of artificial ice systems for magnetic vortices in a superconducting MoGe thin film with patterned nanostructures. *Phys. Rev. Lett.* 111, 067001. doi:10.1103/PhysRevLett.111.067001.
- Laviano, F., Ghigo, G., Mezzetti, E., Hollmann, E., Würdenweber, R., 2010. Control of the vortex flow in microchannel arrays produced in YBCO films by heavy-ion lithography. *Physica C* 470, 844–847. doi:10.1016/j.physc.2010.02.052.
- Lee, C.S., Jankó, B., Derényi, I., Barabási, A.L., 1999. Reducing vortex density in superconductors using the ‘ratchet effect’. *Nature* 400, 337–340. doi:10.1038/22485.
- LeFebvre, J.C., Cho, E., Li, H., Pratt, K., Cybart, S.A., 2019. Series arrays of planar long Josephson junctions for high dynamic range magnetic flux detection. *AIP Adv.* 9, 105215. doi:10.1063/1.5126035.
- Libál, A., Olson Reichhardt, C.J., Reichhardt, C., 2009. Creating artificial ice states using vortices in nanostructured superconductors. *Phys. Rev. Lett.* 102, 237004. doi:10.1103/physrevlett.102.237004.

- Likharev, K.K., 2012. Superconductor digital electronics. *Physica C* 482, 6–18. doi:10.1016/j.physc.2012.05.016.
- Lyu, Y.Y., Jiang, J., Wang, Y.L., Xiao, Z.L., Dong, S., Chen, Q.H., Milošević, M.V., Wang, H., Divan, R., Pearson, J.E., Wu, P., Peeters, F.M., Kwok, W.K., 2021. Superconducting diode effect via conformal-mapped nanoholes. *Nat. Commun.* 12, 2703. doi:10.1038/s41467-021-23077-0.
- Marinković, S., Fernández-Rodríguez, A., Collienne, S., Alvarez, S.B., Melinte, S., Maiorov, B., Rius, G., Granados, X., Mestres, N., Palau, A., Silhanek, A.V., 2020. Direct visualization of current-stimulated oxygen migration in $\text{YBa}_2\text{Cu}_3\text{O}_{7-\delta}$ thin films. *ACS Nano* 14, 11765–11774. doi:10.1021/acsnano.0c04492.
- Markowitsch, W., Stockinger, C., Lang, W., Bierleutgeb, K., Pedarnig, J.D., Bäuerle, D., 1997. Photoinduced enhancement of the c-axis conductivity in oxygen-deficient $\text{YBa}_2\text{Cu}_3\text{O}_{7-\delta}$ thin films. *Appl. Phys. Lett.* 71, 1246–1248. doi:10.1063/1.119863.
- Martin, J.I., Vélez, M., Nogués, J., Schuller, I.K., 1997. Flux pinning in a superconductor by an array of submicrometer magnetic dots. *Phys. Rev. Lett.* 79, 1929–1932. doi:10.1103/PhysRevLett.79.1929.
- Milošević, M.V., Berdiyrov, G.R., Peeters, F.M., 2007. Fluxonic cellular automata. *Appl. Phys. Lett.* 91, 212501. doi:10.1063/1.2813047.
- Misko, V., Savel'ev, S., Nori, F., 2005. Critical currents in quasiperiodic pinning arrays: Chains and Penrose lattices. *Phys. Rev. Lett.* 95, 177007. doi:10.1103/PhysRevLett.95.177007.
- Misko, V.R., Bothner, D., Kemmler, M., Kleiner, R., Koelle, D., Peeters, F.M., Nori, F., 2010. Enhancing the critical current in quasiperiodic pinning arrays below and above the matching magnetic flux. *Phys. Rev. B* 82, 184512. doi:10.1103/PhysRevB.82.184512.
- Misko, V.R., Nori, F., 2012. Magnetic flux pinning in superconductors with hyperbolic-tessellation arrays of pinning sites. *Phys. Rev. B* 85, 184506. doi:10.1103/PhysRevB.85.184506.
- Moshchalkov, V.V., Baert, M., Metlushko, V.V., Rosseel, E., Bael, M.J.V., Temst, K., Jonckheere, R., Bruynseraede, Y., 1996. Magnetization of multiple-quanta vortex lattices. *Phys. Rev. B* 54, 7385–7393. doi:10.1103/physrevb.54.7385.
- Moshchalkov, V.V., Fritzsche, J., 2011. Nanostructured superconductors. World Scientific, Singapore. doi:10.1142/9789814343923.
- Müller, B., Karrer, M., Limberger, F., Becker, M., Schröppel, B., Burkhardt, C.J., Kleiner, R., Goldobin, E., Koelle, D., 2019. Josephson junctions and SQUIDS created by focused helium-ion-beam irradiation of $\text{YBa}_2\text{Cu}_3\text{O}_7$. *Phys. Rev. Applied* 11, 044082. doi:10.1103/PhysRevApplied.11.044082.
- Nelson, D.R., Vinokur, V.M., 1993. Boson localization and correlated pinning of superconducting vortex arrays. *Phys. Rev. B* 48, 13060–13097. doi:10.1103/physrevb.48.13060.
- Parks, R.D., Little, W.A., 1964. Fluxoid quantization in a multiply-connected superconductor. *Phys. Rev.* 133, A97–A103. doi:10.1103/PhysRev.133.A97.
- Pedarnig, J.D., Rössler, R., Delamare, M.P., Lang, W., Bäuerle, D., Köhler, A., Zandbergen, H.W., 2002. Electrical properties, texture, and microstructure of vicinal $\text{YBa}_2\text{Cu}_3\text{O}_{7-\delta}$ thin films. *Appl. Phys. Lett.* 81, 2587–2589. doi:10.1063/1.1508418.
- Perez de Lara, D., Alija, A., Gonzalez, E.M., Velez, M., Martin, J.I., Vicent, J.L., 2010. Vortex ratchet reversal at fractional matching fields in kagomélike array with symmetric pinning centers. *Phys. Rev. B* 82, 174503. doi:10.1103/PhysRevB.82.174503.
- Poccia, N., Baturina, T.I., Coneri, F., Molenaar, C.G., Wang, X.R., Bianconi, G., Brinkman, A., Hilgenkamp, H., Golubov, A.A., Vinokur, V.M., 2015. Critical behavior at a dynamic vortex insulator-to-metal transition. *Science* 349, 1202–1205. doi:10.1126/science.1260507.
- Reichhardt, C., Olson Reichhardt, C.J., 2007. Vortex molecular crystal and vortex plastic crystal states in honeycomb and kagomé pinning arrays. *Phys. Rev. B* 76, 064523. doi:10.1103/PhysRevB.76.064523.
- Reichhardt, C., Ray, D., Olson Reichhardt, C.J., 2015. Reversible ratchet effects for vortices in conformal pinning arrays. *Phys. Rev. B* 91, 184502. doi:10.1103/physrevb.91.184502.
- Savel'ev, S., Nori, F., 2002. Experimentally realizable devices for controlling the motion of magnetic flux quanta in anisotropic superconductors. *Nat. Mater.* 1, 179–184. doi:10.1038/nmat746.
- Sefrioui, Z., Arias, D., González, E.M., León, C., Santamaria, J., Vicent, J.L., 2001. Vortex liquid entanglement in irradiated $\text{YBa}_2\text{Cu}_3\text{O}_{7-\delta}$ thin films. *Phys. Rev. B* 63, 064503. doi:10.1103/PhysRevB.63.064503.
- Silhanek, A.V., Gillijns, W., Moshchalkov, V.V., Zhu, B.Y., Moonens, J., Leunissen, L.H.A., 2006. Enhanced pinning and proliferation of matching effects in a superconducting film with a Penrose array of magnetic dots. *Appl. Phys. Lett.* 89, 152507. doi:10.1063/1.2361172.
- Silhanek, A.V., Van de Vondel, J., Moshchalkov, V.V., 2010. Guided vortex motion and vortex ratchets in nanostructured superconductors, in: Moshchalkov, V.V., Wördenweber, R., Lang, W. (Eds.), *Nanoscience and Engineering in Superconductivity*. Springer, Heidelberg, pp. 1–24. doi:10.1007/978-3-642-15137-8.
- Sochnikov, I., Shaulov, A., Yeshurun, Y., Logvenov, G., Bozovic, I., 2010. Large oscillations of the magnetoresistance in nanopatterned high-temperature superconducting films. *Nat. Nanotechnol.* 5, 516–519. doi:10.1038/nnano.2010.111.
- Swiecki, I., Ulysse, C., Wolf, T., Bernard, R., Bergeal, N., Briatico, J., Faini, G., Lesueur, J., Villegas, J.E., 2012. Strong field-matching effects in superconducting $\text{YBa}_2\text{Cu}_3\text{O}_{7-\delta}$ films with vortex energy landscapes engineered via masked ion irradiation. *Phys. Rev. B* 85, 224502. doi:10.1103/physrevb.85.224502.
- Tafuri, F., 2024. Josephson junctions, in: Chakraborty, T. (Ed.), *Encyclopedia of Condensed Matter Physics (Second Edition)*. Academic Press, Oxford, pp. 616–631. doi:10.1016/B978-0-323-90800-9.00145-1.
- Tafuri, F., Kirtley, J.R., 2005. Weak links in high critical temperature superconductors. *Rep. Progr. Phys.* 68, 2573–2663. doi:10.1088/0034-4885/68/11/r03.
- Tinchev, S.S., 1996. Properties of YBCO weak links prepared by local oxygen-ion induced modification. *Physica C* 256, 191–198. doi:10.1016/0921-4534(95)00615-x.
- Trastoy, J., Malnou, M., Ulysse, C., Bernard, R., Bergeal, N., Faini, G., Lesueur, J., Briatico, J., Villegas, J.E., 2014. Freezing and thawing of artificial ice by thermal switching of geometric frustration in magnetic flux lattices. *Nat. Nanotechnol.* 9, 710–715. doi:10.1038/nnano.2014.158.
- Villegas, J.E., Montero, M.I., Li, C.P., Schuller, I.K., 2006. Correlation length of quasiperiodic vortex lattices. *Phys. Rev. Lett.* 97, 027002. doi:10.1103/physrevlett.97.027002.
- Villegas, J.E., Savel'ev, S., Nori, F., Gonzalez, E.M., Anguita, J.V., García, R., Vicent, J.L., 2003. A superconducting reversible rectifier that controls the motion of magnetic flux quanta. *Science* 302, 1188–1191. doi:10.1126/science.1090390.
- Vinckx, W., Vanacken, J., Moshchalkov, V.V., Mátéfi-Tempfli, S., Mátéfi-Tempfli, M., Michotte, S., Piriaux, L., Ye, X., 2007. High field matching effects in superconducting Nb porous arrays catalyzed from anodic alumina templates. *Physica C* 459, 5–10. doi:10.1016/j.physc.2007.04.194.
- Van de Vondel, J., Silva, C.C.D., Zhu, B.Y., Morelle, M., Moshchalkov, V.V., 2005. Vortex-rectification effects in films with periodic asymmetric pinning. *Phys. Rev. Lett.* 94, 057003. doi:10.1103/PhysRevLett.94.057003.
- Wambaugh, J.F., Reichhardt, C., Olson, C.J., Marchesoni, F., Nori, F., 1999. Superconducting fluxon pumps and lenses. *Phys. Rev. Lett.* 83, 5106–5109. doi:10.1103/physrevlett.83.5106.
- Ward, B.W., Notte, J.A., Economou, N.P., 2006. Helium ion microscope: A new tool for nanoscale microscopy and metrology. *J. Vac. Sci. Techn. B* 24, 2871–2874. doi:10.1116/1.2357967.
- Weber, H.W., 2003. Irradiation, in: Cardwell, D.A., Ginley, D.S. (Eds.), *Handbook of Superconducting Materials*. IOP Publishing, Bristol, pp. 407–418. doi:10.1201/9781420034202.
- Welp, U., Xiao, Z.L., Jiang, J.S., Vlasko-Vlasov, V.K., Bader, S.D., Crabtree, G.W., Liang, J., Chik, H., Xu, J.M., 2002. Superconducting transition and vortex pinning in Nb films patterned with nanoscale hole arrays. *Phys. Rev. B* 66, 212507. doi:10.1103/physrevb.66.212507.
- Wördenweber, R., Dymashevskii, P., Misko, V.R., 2004. Guidance of vortices and the vortex ratchet effect in high- T_c superconducting thin films obtained by arrangement of antidots. *Phys. Rev. B* 69, 184504. doi:10.1103/physrevb.69.184504.
- Xue, C., Ge, J.Y., He, A., Zharinov, V.S., Moshchalkov, V.V., Zhou, Y.H., Silhanek, A.V., Van de Vondel, J., 2018. Tunable artificial vortex ice in nanostructured superconductors with a frustrated kagome lattice of paired antidots. *Phys. Rev. B* 97, 134506. doi:10.1103/PhysRevB.97.134506.
- Yun, S.H., Pedarnig, J.D., Rössler, R., Bäuerle, D., Obradors, X., 2000. In-plane and out-of-plane resistivities of vicinal Hg-1212 thin films. *Appl. Phys. Lett.* 77, 1369–1371. doi:10.1063/1.1289489.